Measurement and Modeling of the Viscosity of (Nitrogen + Carbon Dioxide) Mixtures at Temperatures from (253.15 to 473.15) K with Pressures up to 2 MPa

Kai Humberg[1], **Markus Richter**[1*], **J. P. Martin Trusler**[2], **Roland Span**[1]

[1] *Lehrstuhl für Thermodynamik, Ruhr-Universität Bochum,*

Universitätsstraße 150, D-44780 Bochum, Germany

[2] *Department of Chemical Engineering, Imperial College London, South Kensington Campus,*

London SW7 2AZ, United Kingdom

ABSTRACT

The viscosity of pure nitrogen and of three (nitrogen + carbon dioxide) mixtures was measured over the temperature range from (253.15 to 473.15) K with pressures up to 2 MPa utilizing a rotating-body viscometer. The relative combined expanded uncertainty ($k = 2$) of viscosity was estimated to be between (0.14 and 0.19) % for nitrogen. For the binary mixtures, the uncertainty ranged between (0.19 and 0.39) %. The new data for nitrogen show very good agreement with experimental data from the literature and with recent *ab initio* calculations. The experimental data for the binary mixtures were compared with an Extended Corresponding States (ECS) model as implemented in the NIST REFPROP 9.1 database. The relative deviations of the data from the model were generally found to increase in magnitude with increasing density and ranged between (−2.1 and 0.4) % near the greatest density studied. The experimental data were correlated using

[*] Corresponding author. Tel.: +49-234-32-26395, E-mail: m.richter@thermo.rub.de.

the modified Enskog theory for hard sphere mixtures correct to the second viscosity virial coefficient. In this analysis, the effective hard-sphere diameters determining (a) the zero-density viscosity and (b) the leading term in the radial distribution function at contact were correlated as functions of temperature. The resulting model was found to represent all measured data with absolute relative deviations < 0.3% for the binary mixtures and < 0.2% for the pure fluids. This implies that the model reproduces or predicts respectively all experimental viscosity data within their experimental uncertainties.

Keywords: Binary Mixtures; Carbon Dioxide; Magnetic suspension coupling; Modified Enskog Theory, Nitrogen, Rotating body; Viscometer; Viscosity; Zero-density limit.

1. INTRODUCTION

The optimization of industrial processes so as to minimize energy consumption and greenhouse gas emissions is one of the most important scientific and engineering challenge of our time. Almost all industrial processes involve the transport of fluids, predominantly mixtures, and the sizing of process equipment and pipelines requires knowledge of the transport properties of these systems. For processes involving flue gases, carbon dioxide and nitrogen are often the main constituents of interest. Against this background, the present study focuses on the viscosity of the (CO_2 + N_2) system.

Measurements of the viscosity of pure gaseous carbon dioxide were recently carried out with a new rotating-body viscometer [1]. In the present paper, we report further measurements of the viscosity of pure nitrogen and of three (carbon dioxide + nitrogen) mixtures in the temperature range from (253.15 to 473.15) K at pressures up to 2 MPa carried out with the same instrument. Herewith, the viscosity was determined relative to helium on the basis of the decay rate of a slender cylindrical body rotating inside the measuring cell; this cylindrical body was levitated by a magnetic-suspension coupling, which served as a nearly frictionless bearing. The viscometer was designed in such a way that the viscosity can be measured in the low-density range with a high degree of repeatability. Since the viscosity η of a gas is weakly dependent on the density, the experimental data allow a precise determination of the viscosity in the limit of zero density by means of analysis in terms of the following truncated expansion:

$$\eta(T,\rho) = \eta^{(0)}(T) + \eta^{(1)}(T)\rho\,. \tag{1}$$

Here, η is the viscosity of the fluid (pure or mixed), $\eta^{(0)}$ is the corresponding zero-density viscosity, ρ is the molar density, $\eta^{(1)}$ is the coefficient of molar density, and the ratio $B_\eta = \eta^{(1)}/\eta^{(0)}$ is known as the second viscosity virial coefficient.

The measured viscosities of pure nitrogen are compared with the correlation of Lemmon and Jacobsen [2] and with available literature data. The experimental mixture viscosities are compared with the predictions of the Extended Corresponding States (ECS) model [3] as implemented in the NIST REFPROP 9.1 database [4]; this model is based on Ely and Hanley's work [5] and does not include specific interaction parameters for the (carbon dioxide + nitrogen) system. In a second step, parameters in the modified Enskog theory for hard sphere mixtures, as implemented by Hendl and Vogel [6] for binary gas mixtures, were fitted to the experimental data. This results in accurate representations of $\eta^{(0)}$, $\eta^{(1)}$ and the viscosity η over the full ranges of temperature, density and composition studied in this work.

2. EXPERIMENTAL SECTION

2.1 Apparatus description

For viscosity measurement, a slender cylindrical rotating body was suspended vertically inside a pressure-tight measuring cell employing a magnetic suspension coupling. A detailed description of viscometry using magnetic suspension couplings is given elsewhere [1][7][8][9][10], and only a short outline is presented here.

The magnetic suspension coupling served as a virtually frictionless bearing for the rotation of the cylindrical body around its symmetry axis. With the viscous drag of the fluid surrounding the cylindrical body, the body's rotation was decelerated. For the determination of the logarithmic

damping coefficient D, the rotational speed of the rotating body was measured with an inductively-coupled sensor. The dynamic viscosity η was then determined by

$$\eta = \frac{zD - D_{\mathrm{R}}}{D_{\mathrm{He}}^{(0)} - D_{\mathrm{R}}} \eta_{\mathrm{He}}^{(0)}, \tag{2}$$

which represents a viscosity determination relative to helium as discussed in detail by Schäfer *et al.* [1]. In equation (2), D_{R} is the residual damping constant that corrects the measured value of D for the residual drag in vacuum. The factor z is the nonstationary parameter, which interprets the nonstationary character of the flow as an increase in the moment of inertia of the cylinder due to the rotating fluid as discussed in [8]; here, the nonstationary parameter depends on the density of the surrounding fluid and only weakly on the geometry of the measuring system. Equation (2) can only be applied in the laminar flow regime induced by the rotating body when measuring the viscosity inside the measuring cell. The viscosity determination relative to helium involves the damping at zero density of helium $D_{\mathrm{He}}^{(0)}$ and a reference value for the viscosity of helium at zero density $\eta_{\mathrm{He}}^{(0)}$. The latter value was calculated from a polynomial fit of the *ab initio* data calculated by Cencek *et al.* [11], and the damping at zero density of helium $D_{\mathrm{He}}^{(0)}$ was determined by extrapolating measured damping values of helium to zero density.

The core of our viscometer was installed in a shock-absorbing frame to protect the measuring cell from perturbing vibrations. The diameter of the rotating cylinder was 11 mm, the width of the annulus between the rotating cylinder and the measuring cell was 4.5 mm, and the length of the cylinder was 116 mm. The measuring cell and rotating body make up a coaxial system, which needs to be thoroughly aligned. For this purpose, the measuring cell was mounted underneath a base plate, which was attached to the frame by four adjusting screws. With these screws the angle

of the instrument could be adjusted with a fine resolution of 0.003°. Moreover, a positioning device was placed on top of the base plate to enable accurate positioning of the rotating body inside the measuring cell in steps of 30 μm.

The measuring cell was fabricated from a titanium alloy (Ti6Al4V) which has a low electrical conductivity of approximately $0.6 \cdot 10^{-6}$ $(\Omega \cdot m)^{-1}$ at T = 273.15 K. Thus, disturbing eddy currents induced by the inhomogeneity of the magnetic field of the rotating permanent magnet were comparatively weak. As a result, the residual damping measured in the evacuated measuring cell was minimized, and the influence of the measured residual drag on the damping value was generally less than 3%. The measuring cell was thermostated by a custom two-stage thermostat housed in a cylinder made of PVC and coated with thermal insulation from the inside (see [1] for further details). To evacuate the measuring cell, a turbo molecular pump was used. Two vacuum sensors were used to measure the vacuum pressure up- and down-stream of the measuring cell.

The thermometry chain of the measuring cell consisted of an AC resistance bridge (ASL, UK, type: F17) and a Pt-100 Ω sensor (calibrated on ITS-90), which was directly contacted with the measuring cell on the same level as the rotating body. Due to temperature gradients along the measuring cell wall and temperature oscillations over time, the expanded uncertainty (k = 1.73) in temperature was 104 mK at T = 253.15 K increasing to 162 mK at T = 473.15 K. We measured the pressure using a vibrating-quartz-crystal-type pressure transducer with a range of 3.45 MPa (Paroscientific, USA, type: 1500A-01), which was calibrated with a gas piston gauge (Fluke Calibration, USA, type: PG-7601) from ambient pressures up to 0.7 MPa. The expanded uncertainty (k = 1.73) of the pressure measurement was 3.5 hPa. An air thermostat was utilized to obtain a constant temperature of 323.15 K for the filling manifold that included the pressure

transducer. The tubing connection between the manifold and the core apparatus was thermostated at the same temperature using electric trace heaters.

2.2 Experimental material

The three binary (nitrogen + carbon dioxide) mixtures under study were prepared gravimetrically according to metrological standards. Our sample preparation procedure as well as the mixture preparation system were described in detail in Section 6 of the doctoral dissertation of Schäfer [7]. The pure substances, which were used for the measurements and to prepare the gas mixtures are described in table 1; we used the pure substances as received, and no additional gas analysis or purification was carried out. We prepared the gas mixtures in 20 L aluminum cylinders (Scott Specialty Gases) supplied with specially treated interior surfaces (Aculife inerting, Scott Specialty Gases [12]). This treatment is supposed to maintain a long-term stability of the mixture compositions. The compositions, molar masses and compositional uncertainties of each mixture are listed in table 2.

2.3 Experimental procedures

For accurate viscosity measurements, concentric alignment of the rotating body and measuring cell is required and the alignment procedure, detailed in [1], was repeated before the present measurements were started. For the damping measurements required during this adjustment, helium gas was used at T = 298.15 K and p = 0.2 MPa.

The isotherms studied were, in the order measured, T = (298.15, 323.15, 373.15, 423.15, 473.15, 253.15, 273.15 and 298.15) K; this sequence included repeated measurements at T = 298.15 K to permit a check on repeatability. For pure nitrogen, the filling procedure described in [1] was used,

whereby the measuring cell was filled separately for every single state point along an isotherm. The procedure was as follows: (1) reduce the pressure of the remaining fluid down to atmospheric pressure; (2) refill the measuring cell to p = 2 MPa; (3) reduce to atmospheric pressure and refill again to p = 2 MPa; (4) reduce the pressure to the next measurement point. After the pressure was adjusted, a period of 15 minutes was allowed for equilibration before the measurements were started. In order to conserve material, a different procedure was used for the mixtures. Initially, the measuring cell was flushed at the desired temperature and at a constant pressure of about 0.2 MPa for 15 minutes. The volumetric flow rate used was such that two or three times the system volume was passed through the cell. Then the pressure was increased to the desired greatest pressure for the isotherm and measurements proceeded along the isotherm of interest with decrements in pressure without refilling the measuring cell.

In between measurements with different fluid composition, the measuring cell was evacuated using a turbo molecular pump for at least twelve hours at a temperature of 373.15 K. This was followed by three cycles of filling to p = 0.2 MPa followed by evacuation for 15 minutes, then filling to p = 1 MPa and cooling to T = 298.15 K before finally venting and filling as explained above.

As detailed in reference [1], the rotating body was initially accelerated to a rotational frequency of 205 mHz (12.3 rpm) and the damping measurement did not commence until the body had slowed to a rotational frequency of 200 mHz (12 rpm), thereby allowing time for the establishment of a pseudo-steady-state flow regime. Measurements were performed only when laminar disk flow above and below the rotating body and laminar couette flow in the annulus between the rotating body and the measuring cell could be assured. To verify that this was the case, the Reynolds number for the disk flow and the Taylor number for the flow in the annulus were calculated at the maximum rotational frequency for every state point investigated. The duration of a single damping

measurement was 9 minutes and, in all cases, an average value of at least three successive damping measurements was used to determine the viscosity. The temperature and pressure ascribed to the mean viscosity were the mean of the values recorded during the measurements at the state point in question.

3. RESULTS

3.1 Uncertainty analysis

The uncertainty analysis given in [1], which is based on the Guide to the Expression of Uncertainty in Measurement [13], was adapted to the current work. The uncertainty budget for an exemplary temperature of 473.15 K for the (0.75 CO_2 + 0.25 N_2) mixture is listed in table 3. The main contribution to this uncertainty arose from the determination of the damping D, the residual damping D_R, and the damping at zero density of helium $D_{He}^{(0)}$. The uncertainties of these input parameters as well as the parameters collected under the term "Rest" are fully detailed in [1]. The uncertainty budgets of D, $D_{He}^{(0)}$ and the combined uncertainties including temperature, pressure and composition are again listed in tables (4 to 6) exemplarily for the (0.75 CO_2 + 0.25 N_2) mixture at T = 473.15 K. The expanded combined uncertainty (k = 2) in viscosity for all data points varies from (0.025 to 0.066) μPa·s, and the corresponding relative expanded combined uncertainty (k = 2) ranges from (0.14 to 0.39) %.

In this work, we paid particular attention to the uncertainty arising from composition changes associated with sorption. To estimate the expanded uncertainty (k = 1.73) $U_{sorption}(D)$, we measured the damping of each mixture at the same state point (T = 298.15 K and p = 0.2 MPa) several times over a time period of at least two days. Note that, according to the "Guide to the Expression of Uncertainty in Measurement" [13], estimations of measurement deviations, e.g.,

sorption effects or temperature gradients, are described by a symmetric, rectangular probability distribution, thus, the coverage factor was assumed to be $k = \sqrt{3} \approx 1.73$. During this period, damping measurements were taken with and without flushing the cell, and we observed that the damping values decrease slightly over a period of approximately two hours, which we attribute to desorption of carbon dioxide from soft seal materials. We estimated an average slope with respect to time of the damping values and calculated the change in the damping values that occurs over a period of about nine hours, which is the typical time required to measure one isotherm. For the measurements on pure nitrogen, no sorption effects were observed.

3.2 Measurements on nitrogen

The viscosity of nitrogen was measured at 56 state points (including reproducibility checks at T = 298.15 K and T = 323.15 K) along seven isotherms at T = (253.15, 273.15, 298.15, 323.15, 373.15, 423.15, 473.15) K with pressures up to 1.8 MPa. The experimental results are listed in table 7. To obtain values for the viscosity in the limit of zero density and the second viscosity virial coefficient, the data were analyzed by linear regression with equation (1) making use of densities computed from the equation of state of Span *et al.* [14]. The resulting values for $\eta_{\mathrm{exp}}^{(0)}$ and B_η are listed in table 8.

Numerous authors have measured the viscosity of nitrogen before, and here we compare our data with the selected experimental viscosity data from the literature listed in table 9. We compare our measured data as well as the experimental data of other authors with the correlation of Lemmon and Jacobsen [2] and the relative deviations from that correlation are plotted versus molar density in figures 1 and 2. The relative uncertainty of the correlation of Lemmon and Jacobsen was reported to be 0.5% in the dilute gas increasing up to 2% at high pressures. If not included with

the published data, we calculated the corresponding densities from the equation of state of Span *et al.* [14] for the purpose of data comparison.

At T = 253.15 K, we observe relative deviations varying from −0.3% at a density of 0.02 mol·l^{-1} to −0.1% at ρ = 0.57 mol·l^{-1} (see figure 1 (a)). This trend is less pronounced at T = 273.15 K as can be seen in figure 1 (b). Figure 1 (c), at T = 298.15 K, illustrates that the relative deviations of the present data are almost constant at approximately −0.2%. For higher temperatures, the relative deviations of the present data from the correlation of Lemmon and Jacobsen [2] are almost independent of density along each isotherm, as shown in figure 1 (d) and figure 2, and they vary from approximately −0.3% at T = 323.15 K to −0.6% at T = 473.15 K. Hence, all measured data points are within the uncertainty of the correlation of Lemmon and Jacobsen [2].

Overall, we observe slightly lower viscosities than the average of the data of other authors. Nevertheless, the present data agree well with selected recent literature data. At T = 298.15 K and ρ = 0.08 mol·l^{-1}, the absolute relative deviation from the measured viscosity of May *et al.* [25] is < 0.01%. In the same density region, absolute relative deviations of our data from the viscosities of Vogel [28] and Seibt *et al.* [26] are no more than 0.1%.

For densities higher than 0.08 mol·l^{-1} at T = 298.15 K, we observe good agreement with data of Seibt *et al.* [27] and, for the highest measured densities, with Seibt *et al.* [26] and Kestin *et al.* [22]. For T = 323.15 K, our results are close to the data of Seibt *et al*. [26] and Seibt *et al*. [27]. For all isotherms above T = 323.15 K, greater scatter can be observed among the viscosity data reported by other authors at atmospheric pressure. For T = 373.15 K and T = 473.15 K, the present data agree with Vogel's [28] data within the experimental uncertainty.

As shown in figure 3, our extrapolated zero-density viscosities show very good agreement with the *ab initio* calculations of Hellmann *et al.* [29], which are scaled by a factor of 1.0024 as suggested in reference [30]. Accordingly, the deviations of the non-scaled values of Hellmann *et al.* [29] are higher and slightly out of the range of the experimental uncertainties of the present work. The trend of the relative deviations from the correlation of Lemmon and Jacobsen [2] also follows the behavior of the data of Vogel [28] and, for temperatures higher than 373.15 K, the data of Seibt *et al.* [26]. The relative deviations from the values of Berg and Moldover [31] and May *et al.* [25] at T = 298.15 K are just 0.04%.

3.3 Measurements on mixtures

The viscosity of three (carbon dioxide + nitrogen) mixtures was measured at 157 (T, p) state points (including reproducibility checks at T = 298.15 K) along seven isotherms at T = (253.15, 273.15, 298.15, 323.15, 373.15, 423.15, 473.15) K with pressures up to 2.0 MPa. The reported viscosity values are the average of five successive measurements over a period of about 45 minutes. The related temperature and pressure values are average values taken over this time.

The experimental results are listed in table 10. The corresponding density was calculated from the GERG-2008 equation of state [33] as implemented in the NIST REFPROP 9.1 database [4]. Relative deviations between the measured viscosities and values estimated from an extended corresponding states (ECS) model are shown as a function of molar densities in figure 4 (a) to (c). For this purpose, the ECS model implemented in the NIST REFPROP 9.1 database was used [3]. This model is based on reference [5] and does not include specific interaction parameters for the (carbon dioxide + nitrogen) mixture. For the mixture with x_{N_2} = 0.75, the comparisons in figure 4 (a) show negative relative deviations to the calculated values which increase with density up to

about −2.1%. In the case of the equimolar mixture, the relative deviations, shown in figure 4 (b), are again negative but of smaller magnitude, reaching −0.5% at 473.15 K. Finally, for the carbon dioxide-rich mixture, the relative deviations plotted in see figure 4 (c) have a positive trend with increasing density for all isotherms and vary from about −0.4% at $\rho = 0.03$ mol·l^{-1} and $T = 473.15$ K to 0.4% at $\rho = 0.58$ mol·l^{-1} and $T = 373.15$ K.

At temperatures near 300 K, Kestin and Leidenfrost [34], Kestin and Ro [35] and Kestin *et al.* [21] each measured the viscosity of binary (carbon dioxide + nitrogen) mixtures with an oscillating disc viscometer. Kestin and Leidenfrost [34] claim an uncertainty of 0.05%, while Kestin and Ro [35] and Kestin *et al.* [21] claim 0.1%. In figure 5 (a) to (c), relative deviations of the present data at $T = 298.15$ K from the REFPROP ECS model are plotted versus the molar density together with data of Kestin and Leidenfrost [34], Kestin and Ro [35] and Kestin *et al.* [21]. These comparisons show a good level of mutual agreement over wide ranges of density and composition.

Figure 6 shows relative deviations of the extrapolated zero-density viscosities, as well as the *ab initio* calculated zero-density viscosity values of Crusius *et al.* [36], from the REFPROP ECS model for all mixtures as a function of temperature. For extrapolation, we used equation (1) and the results, listed in table 11, show a worst-case relative deviation from the REFPROP ECS model of −0.7% for the mixture with $x_{N_2} = 0.75$ at $T = 473.15$ K. The relative deviations are smaller in magnitude for the equimolar mixture and the mixture with $x_{N2} = 0.25$. Compared with the *ab initio* values of Crusius *et al.* [36], the present data agree to within the experimental uncertainty in almost all cases with deviations between 0.1% and 0.3%.

4. MODELING

4.1 Theory

The kinetic theory of moderately-dense real-gas mixtures has been developed by Di Pippo *et al.* [37] and described in detail by Kestin *et al*. [38], Vesovic and Wakeham [39][40] and Hendl and Vogel [6][41]. This approach is based upon a modification of the Thorne-Enskog theory for mixtures of hard spherical molecules, according to which the leading terms in equation (1) for the density expansion of the viscosity of a binary mixture are:

$$\eta_{\mathrm{mix}}^{(0)} = \left[x_1^2 H_{22}^{(0)} + x_2^2 H_{11}^{(0)} - 2x_1 x_2 H_{12}^{(0)}\right]\left[H_{11}^{(0)} H_{22}^{(0)} - H_{12}^{(0)^2}\right]^{-1} \tag{3}$$

$$\eta_{\mathrm{mix}}^{(1)} = \left[x_1^2 H_{22}^{(1)} + x_2^2 H_{11}^{(1)} - 2x_1 x_2 H_{12}^{(1)} + 2x_1 y_1^{(1)} H_{22}^{(0)} + 2x_2 y_2^{(1)} H_{11}^{(0)} - 2x_1 y_2^{(1)} H_{12}^{(0)} - 2x_2 y_1^{(1)} H_{12}^{(0)} - \eta_{\mathrm{mix}}^{(0)}\left(H_{11}^{(0)} H_{22}^{(1)} + H_{11}^{(1)} H_{22}^{(0)} - 2H_{12}^{(0)} H_{12}^{(1)}\right)\right]\left[H_{11}^{(0)} H_{22}^{(0)} - H_{12}^{(0)^2}\right]^{-1} \tag{4}$$

Here, $H_{ij}^{(k)}$ are a set of matrix elements, x_i is the mole fraction of component *i*, and $y_i^{(1)}$ is given by

$$y_i^{(1)} = \frac{4}{5} x_i \sum_{j=1}^{2} \frac{m_j}{m_i + m_j} x_j b_{ij} \tag{5}$$

where m_i is the mass of molecule *i*, b_{ij} is a molar co-volume,

$$b_{ij} = \frac{2}{3}\pi N_{\mathrm{Av}} \sigma_{ij}^3 , \tag{6}$$

N_{A} is Avagadro's constant,

$$\sigma_{ij} = \frac{1}{2}\left(\sigma_i + \sigma_j\right) , \tag{7}$$

and σ_i is the diameter of molecule *i*. The matrix elements $H_{ij}^{(k)}$ are given as follows:

$$H_{ii}^{(0)} = \frac{x_i^2}{\eta_i^{(0)}} + \sum_{j=1,j\neq i}^{2} \frac{2x_i x_j}{\eta_{ij}^{(0)}} \frac{m_i m_j}{(m_i+m_j)^2}\left(\frac{5}{3A_{ij}^*} + \frac{m_j}{m_i}\right) \tag{8}$$

$$H_{ii}^{(1)} = \frac{x_i^2 \chi_{ii}^{(1)}}{\eta_i^{(0)}} + \sum_{j=1,j\neq i}^{2} \frac{2x_i x_j \chi_{ij}^{(1)}}{\eta_{ij}^{(0)}} \frac{m_i m_j}{(m_i+m_j)^2}\left(\frac{5}{3A_{ij}^*} + \frac{m_j}{m_i}\right) \tag{9}$$

$$H_{ij}^{(0)}(j\neq i) = -\frac{2x_i x_j}{\eta_{ij}^{(0)}} + \frac{m_i m_j}{(m_i+m_j)^2}\left(\frac{5}{3A_{ij}^*} - 1\right) \tag{10}$$

$$H_{ij}^{(1)}(j\neq i) = -\frac{2x_i x_j \chi_{ij}^{(1)}}{\eta_{ij}^{(0)}} + \frac{m_i m_j}{(m_i+m_j)^2}\left(\frac{5}{3A_{ij}^*} - 1\right) \tag{11}$$

where $\eta_i^{(0)}$ and $\eta_{ij}^{(0)}$ are pure-component and interaction viscosities in the dilute-gas limit, which are given in elementary kinetic theory by

$$\eta_i^{(0)} = \frac{5}{16}\frac{(\pi m_i kT)^{1/2}}{\pi\sigma_i^2} \tag{12}$$

$$\eta_{ij}^{(0)} = \frac{5}{16}\frac{(\pi m_{ij} kT)^{1/2}}{\pi\sigma_{ij}^2} \tag{13}$$

$$m_{ij} = \frac{2m_i m_j}{(m_i+m_j)} \tag{14}$$

The quantity A_{ij}^*, which appears here, is a dimensionless ratio of collision integrals, which is exactly unity for hard spheres. Finally, $\chi_{ij}^{(1)}$ is the coefficient of ρ in the density expansion of the unlike radial distribution function at contact, which is given by

$$\chi_{ij}^{(1)} = \zeta_3 + \frac{3\sigma_{ii}\sigma_{jj}}{2\sigma_{ij}}\zeta_3 \tag{15}$$

$$\zeta_k = \frac{\pi}{6} N_A \sum_{i=1}^{2} x_i \sigma_{ii}^k \,. \tag{16}$$

Equations (3 to 16) serve to evaluate the viscosity of a binary hard-sphere gas correct to leading order in the density. In order to apply these relations to real gases, A_{ij}^* is assigned the value 1.1,

based on the principle of corresponding states, $\eta_i^{(0)}$ is replaced by the experimental dilute-gas viscosities of the pure components, and the molar co-volume b_{ij} is replaced by

$$b_{ij} = B_{ij} + T(dB_{ij}/dT)\,, \tag{17}$$

where B_{ij} is the pure-component ($i = j$) or interaction ($i \neq j$) second pressure virial coefficient. Additionally, it is necessary to adopt effective values, denoted σ_{ij}^{χ}, for the hard-sphere diameters that appear in the expression for $\chi_{ij}^{(1)}$. In the present work, we follow Hendl and Vogel [6] and adopt the arithmetic-mean combining rule, equation (7), for σ_{12}^{χ} and treat σ_{11}^{χ} and σ_{22}^{χ} as adjustable parameters in our analysis. The viscosity of the real-gas mixture is then given correct to first-order in the density by combining equations (3) and (4).

4.2 Application to mixtures

For the application to the (carbon dioxide + nitrogen) mixtures, the second pressure virial coefficients of the pure fluids B_i as well as the second interaction pressure virial coefficient B_{ij} are needed. To describe the temperature dependent pressure virial coefficients of the pure fluids B_i, an equation of the form

$$B_i = \alpha_i + \beta_i \exp(\gamma_i / T) \tag{18}$$

was fitted to experimental data taken from [43], where α, β and γ are the fitted parameters. The molar co-volume b_i is then given by

$$b_i = \alpha_i + \beta_i[1-(\gamma_i / T)]\exp(\gamma_i / T)\,. \tag{19}$$

For the fitting procedure, we used the experimental data in the temperature range from (200 to 523.15) K for nitrogen and (217 to 523.20) K for carbon dioxide. The resulting parameters are listed in table 12. The available literature for the second interaction virial coefficient was found to be rather limited and insufficient to permit reliable determination of the parameters in equation (19). Therefore, a simple arithmetic mean rule was followed for calculating b_{ij}:

$$b_{ij} = \frac{1}{2}\left(b_i + b_j\right) \tag{20}$$

The zero-density viscosity of nitrogen and the binary mixtures was taken from the present work, while that of carbon dioxide was obtained from our previous study [1]. Since Hendl and Vogel [6] found that the simultaneous fitting of σ_i^{χ} to the experimental data of both pure substances and of one mixture leads to the best results, only this approach was applied here. We used the experimental data of the equimolar mixture for this procedure. The interaction term, σ_{ij}^{χ}, was not adjusted separately and was instead obtained from the combining rule expressed in equation (7). The fitting was accomplished in two steps. In the first step, starting with equations (12) and (13), we fitted the coefficients $a_{i,k}$ in the polynomial functions

$$\sigma_i^0 = \sum_{k=0}^{n} a_{i,k} T^k \tag{21}$$

that describe the temperature dependence of the effective diameters σ_i^0 of the pure fluids as an interaction parameter L_{12} in the following combining rule for σ_{ij}^0:

$$\sigma_{ij}^0 = \frac{1 - L_{12}}{2}\left(\sigma_i^0 + \sigma_j^0\right) \tag{22}$$

It was found that third order polynomial functions (n = 3) provided a good representation of the data and the resulting coefficients are listed in table 13. Relative deviations of the experimental

zero-density-viscosities from the values calculated from equations (12) and (13) together with equations (21) and (22) are shown in figure 7. The maximum absolute relative deviation is 0.13%, which implies that every data point is represented within its standard uncertainty. In the second step of the fitting, the effective diameters σ_i^{χ} were represented as functions of temperature by means of the polynomial functions,

$$\sigma_i^{\chi} = \sum_{k=0}^{n} b_{i,k} T^k \,, \tag{23}$$

and the interaction term σ_{12}^{χ} was obtained from the combining rule, equation (7), without a binary parameter. The coefficients $b_{i,k}$ were then fitted to the experimental data for $\eta^{(1)}$ for every isotherm for both the pure fluids and the equimolar mixture. In this case, quadratic functions of temperature (n = 2) were sufficient, and the resulting coefficients are given in table 13.

Having obtained the parameters as detailed above, we proceeded to compare the original viscosity data with the model. Relative deviations of the data from the model are shown as a function of molar density in figure 8, for the mixtures, and figure 9 for the two pure components. Up to a density of approximately 0.3 mol·l^{-1}, the deviations from the model are almost independent of ρ and a maximum absolute relative deviation of 0.2% can be observed. At higher densities, the deviations for the three binary mixture compositions have a slight negative trend with increasing density, reaching about −0.3% in the worst case. This is not observed for pure nitrogen, and the data for pure carbon dioxide do not extend beyond ρ = 0.3 mol·l^{-1}. Overall, it can be concluded that the model reproduces or predicts all the experimental viscosity data within their uncertainties. Thus, the proposition of Hendl and Vogel [6] that the model can correlate accurately binary mixture viscosities in the low-density range can be confirmed.

4. CONCLUSION

In this study, we extended our earlier work [1] on the viscosity of pure carbon dioxide at low density to encompass the viscosity of pure nitrogen and of three mixtures of carbon dioxide and nitrogen. The measurements, relative to helium, were made for mixtures with nominal CO_2 mole fraction of 0.00, 0.25, 0.50 and 0.75 along seven isotherms between (253.15 and 473.15) K at pressures up to 2 MPa. The relative expanded combined uncertainty in viscosity (k = 2) ranged from (0.14 to 0.19) % for nitrogen and from (0.19 to 0.39) % for the binary mixtures. The results for the viscosity of nitrogen have been compared with the correlation of Lemmon and Jacobsen [2] and to selected literature data. The average deviation of the present data from the correlation of Lemmon and Jacobsen [2] is −0.26% near room temperature. Therefore, the uncertainty of the correlation, which was reported to be 0.5% in the dilute gas, was confirmed. The comparison with literature data showed very good agreement; in particular, the relative deviation from the reference value of Berg and Moldover [31] at T = 298.15 K is just −0.04%. Over wide ranges of temperature and pressure, the present data agree well with experimental data of Vogel [28] and Seibt *et al.* [26][27].

The results for the three (carbon dioxide + nitrogen) mixtures have been compared to values estimated from an extended corresponding states model implemented in the NIST REFPROP 9.1 database [3]. The relative deviations were found to increase in magnitude with increasing density, reaching about −2.1% at the highest density studied. In the limit of zero density, the worst case relative deviation from the model was about −0.7%. The correlation scheme developed by Hendl and Vogel [6], based on the modified Enskog theory, was parameterized for the carbon dioxide-nitrogen system on the basis of the experimental data. This correlation described all experimental

data within their experimental uncertainties. The worst-case relative deviation of the experimental data from the model was −0.3%.

Acknowledgements

We thank the Deutsche Forschungsgemeinschaft for funding this project under Grant No. SP 507/10-2. This work was supported by the Ruhr-University Research School PLUS, funded by Gemany's Excellence Initiative [DFG GSC 98/3]. We also thank Dr. Michael Schäfer for his helpful advices during the nitrogen measurements and the mixture sample preparation. Moreover, we are thankful to Andrej Gorochow and Halil Sali for supporting the present project within the scope of their Master's theses. We also thank Dr. Johann-Philipp Crusius and co-workers for providing their *ab initio* viscosity data for the (carbon dioxide + nitrogen) mixtures prior to publication.

LITERATURE CITED

[1] M. Schäfer, M. Richter, R. Span, J. Chem. Thermodyn. 89, 7-15 (2015).

[2] E.W. Lemmon, R.T. Jacobsen, Int. J. Thermophys., 25(1):21-69, 2004.

[3] J.C. Chichester, M.L. Huber, Documentation and Assessment of the Transport Property Model for Mixtures Implemented in NIST REFPROP (Version 8.0), NIST, Boulder, 2008.

[4] E.W. Lemmon, M.L. Huber, M.O. McLinden, Refprop 9.1, NIST Standard Reference Database 23, NIST, Boulder, 2013.

[5] J.F. Ely, H.J.M. Hanley, Ind. Eng. Chem. Fundam. 20(4), 323-332, 1981.

[6] S. Hendl, E. Vogel, Int. J. Thermophys., Vol. 16, No. 5, 1995.

[7] M. Schäfer, Improvements to Two Viscometers Based on a Magnetic Suspension Coupling and Measurements on Carbon Dioxide. PhD thesis, Ruhr-Universität Bochum, Bochum, Germany, 2015. (Available online: http://hss-opus.ub.ruhr-uni-bochum.de/opus4/files/4542/diss.pdf)

[8] A. Docter, H.W. Lösch, W. Wagner, Fortschr.-Ber, VDI-Z, Ser. 3, No 494, 1997.

[9] C. Evers, H.W. Lösch, W. Wagner, Int. J. Thermophys. 23, 1411-1439, 2002.

[10] T. El Hawary, Messung der Dichte und Viskosität in der Gasphase von Methan, Stickstoff und Methan-Stickstoff-Gemischen mit einer weiterentwickelten kombinierten Viskositäts-Dichte-Messanlage und einer neuen Viskositätsmessanlage für geringe Gasdichten (Measurement of the density and the viscosity in the gas phase of methane, nitrogen and methane-nitrogen mixtures utilizing a modified combined viscometer-densimeter and a new viscometer for low gas densities). PhD thesis, Ruhr-Universität Bochum, Bochum, Germany, 2009. (Available online: http://www-brs.ub.ruhr-uni-bochum.de/netahtml/HSS/Diss/HawaryTarekel/diss.pdf)

[11] W. Cencek, M. Przybytek, J. Komasa, J.B. Mehl, B. Jeziorski, K. Szalewicz, J. Chem. Phys. 136 (2012) 224303.

[12] Scott Specialty Gases Netherlands B.V., Gas cylinders with Aculife treatment, http://scottgas.com/ (accessed 20.12.2017).

[13] ISO International Organization for Standardization, Uncertainty of measurement - Part3: Guide to the expression of uncertainty in measurement, 2008.

[14] R. Span, E.W. Lemmon, R.T. Jacobsen, W. Wagner, A. Yokozeki, J. Phys. Chem. Ref. Data, 29(6): 1361-1433, 2000.

[15] A.G. Clarke, E.B. Smith, J. Chem. Phys. 51(9), 4156-4161, 1969.

[16] R. DiPippo, J. Kestin, K. Oguchi, J. Chem. Phys. 46(12), 4758-4764, 1967.

[17] G.P. Flynn, R.V. Hanks, N.A. Lemaire, J. Ross, J. Chem. Phys. 38, 154-162, 1963.

[18] D.W. Gough, G.P. Matthews, E.B. Smith, J. Chem. Soc. Faraday Trans. 1 72, 645-653, 1976.

[19] J.A. Gracki, G.P. Flynn, J. Ross, J. Chem. Phys. 51, 3856-3863, 1969.

[20] J.M. Hellemans, J. Kestin, S.T. Ro, J. Chem. Phys. 57, 4038-4042, 1972.

[21] J. Kestin, Y. Kobayashi, R.T. Wood, Physica 32, 1065-1089, 1966.

[22] J. Kestin, E. Paykoc, J.V. Sengers, Physica 54, 1-19, 1971.

[23] J. Kestin, S.T. Ro, W.A. Wakeham, J. Chem. Phys. 56, 5837-5842, 1972.

[24] J. Kestin, H.E. Khalifa, S.T. Ro, W.A. Wakeham, Physica 88A, 242-260, 1977.

[25] E.F. May, M.R. Moldover, R.F. Berg, Int. J. Thermophys. 28, 1085-1110, 2007.

[26] D. Seibt, E. Vogel, E. Bich, D. Buttig, E. Hassel, J.Chem. Eng. Data 51, 526-533, 2006.

[27] D. Seibt, S. Herrmann, E. Vogel, E. Bich, E. Hassel, J. Chem. Eng. Data 54, 2626-2637, 2009.

[28] E. Vogel, Int. J. Thermophys. 33, 741-757, 2012.

[29] R. Hellmann, Mol. Phys. 111(3), 387-401, 2013.

[30] R. Hellmann, E. Bich, E. Vogel, V. Vesovic, J. Chem. Phys 141, 224301, 2014.

[31] R.F. Berg, M.R. Moldover, J. Phys. Chem. Ref. Data 41 (2012) 043104.

[32] W.A. Cole, W.A. Wakeham, J. Phys. Chem. Ref. Data 14(1), 209-226, 1985.

[33] O. Kunz, W. Wagner, J. Chem. Eng. Data 57, 3032-3091, 2012.

[34] J. Kestin, W. Leidenfrost, Physica 25, 525-536, 1959.

[35] J. Kestin, S.T. Ro, Ber. Bunsenges. Phys. Chem. 78, 20-24, 1974.

[36] J.-P. Crusius, R. Hellmann, J.C. Castro-Palacio, V. Vesovic, paper in preparation.

[37] R. Di Pippo, J.R. Dorfman, J. Kestin, H.E. Khalifa, E.A. Mason, Physica 86A, 205-223, 1977.

[38] J. Kestin, Ö. Korfali, J.V. Sengers, B. Kamgar-Parsi, Physica 106A, 415-442, 1981.

[39] V. Vesovic, W.A. Wakeham, Chem. Eng. Sci. 44(10), 2181-2189, 1989.

[40] V. Vesovic, W.A. Wakeham, Int. J. Thermophys. 10(1), 125-132, 1989.

[41] S. Hendl, E. Vogel, High Temp. High Press. 25, 279-289, 1993.

[42] R. Span, W. Wagner, J. Phys. Chem. Ref. Data 25, 1509–1596, 1996.

[43] J.H. Dymond, K.N. Marsh, R.C. Wilhoit, K.C. Wong, Virial Coefficients of Pure Gases, Part A, Landolt-Börnstein, New Series IV/21A, 2002.

[44] E. Vogel, Int. J. Thermophys. 37:63, 2016.

TABLES

Table 1. Description of chemical samples, where *x* denotes mole fraction purity.

Chemical	Source	Purity *x*	Additional Purification
Carbon dioxide	Air Liquide, Germany	0.999 995 [a]	None
Nitrogen	Air Liquide, Germany	0.999 999 [b]	None

[a] Impurities stated by the supplier: $x(H_2O) \leq 2.0 \cdot 10^{-6}$, $x(O_2) \leq 1.0 \cdot 10^{-6}$, $x(C_mH_n) \leq 0.1 \cdot 10^{-6}$, $x(N_2) \leq 2.0 \cdot 10^{-6}$, $x(CO) \leq 0.5 \cdot 10^{-6}$, $x(NO_x) \leq 0.1 \cdot 10^{-6}$.

[b] Impurities stated by the supplier: $x(H_2O) \leq 0.5 \cdot 10^{-6}$, $x(O_2) \leq 0.1 \cdot 10^{-6}$, $x(C_mH_n) \leq 0.1 \cdot 10^{-6}$, $x(CO) \leq 0.1 \cdot 10^{-6}$, $x(CO_2) \leq 0.1 \cdot 10^{-6}$, $x(H_2) \leq 0.1 \cdot 10^{-6}$.

Table 2. Compositions (mole fractions x_{CO_2} of CO_2), mean molar mass M, and expanded uncertainty in composition, $U(x_{CO2})$ ($k = 2$), of the prepared mixtures.

	Mixture		
	1	2	3
x_{CO_2}	0.75212	0.50038	0.25019
M/(g·mol^{-1})	40.045	36.018	32.016
$U(x_{CO_2})$ ($k = 2$)	$1.4 \cdot 10^{-4}$	$8.0 \cdot 10^{-5}$	$2.0 \cdot 10^{-5}$

Table 3. Budget for the uncertainty[a] in viscosity at a temperature of 473.15 K for the (0.75 carbon dioxide + 0.25 nitrogen) mixture.

Source of uncertainty	Uncertainty	Distribution	Coverage factor	Sensitivity coefficient	Standard uncertainty
Damping	2.430 μHz	normal	2	0.0221 Pa·s^2	0.02688 μPa·s
Residual damping	8.819 μHz	rectangular	1.73	0.0030 Pa·s^2	0.01519 μPa·s
Damping at zero density of helium	0.899 μHz	rectangular	1.73	0.0191 Pa·s^2	0.00995 μPa·s
Rest					0.00223 μPa·s
Expanded uncertainty (k = 2)				0.065 μPa·s	

[a] The expanded uncertainty in viscosity for the (0.75 carbon dioxide + 0.25 nitrogen) mixture ranges from (0.041 to 0.065) μPa·s, depending on temperature.

Table 4. Budget for the uncertainty[a] of the damping D at a temperature of 473.15 K for the (0.75 carbon dioxide + 0.25 nitrogen) mixture.

Source of uncertainty	Uncertainty	Distribution	Coverage factor	Sensitivity coefficient	Standard uncertainty
Regression	0.022 μHz	normal	2	1	0.01 μHz
Scatter	$0.001 \cdot D$	normal	2	1	0.54 μHz
Hysteresis	0.29·0.40 μHz	rectangular	1.73	1	0.07 μHz
Sorption	$0.0017 \cdot D$	rectangular	1.73	1	1.07 μHz
Change in eccentricity	0.324 μHz	rectangular	1.73	1	0.18 μHz
Expanded uncertainty (k = 2)				2.43 μHz	

[a] The expanded uncertainty ranges from (1.39 to 2.43) μHz, depending on temperature for the (0.75 carbon dioxide + 0.25 nitrogen) mixture.

Table 5. Budget for the uncertainty of the damping at zero density of helium $D_{\mathrm{He}}^{(0)}$ at a temperature of 473.15 K.

Source of uncertainty	Uncertainty	Distribution	Coverage factor	Sensitivity coefficient	Standard uncertainty
Extrapolation	0.47 μHz	rectangular	1.73	1	0.27 μHz
Hysteresis	0.40 μHz	rectangular	1.73	1	0.23 μHz
Regression	0.02 μHz	rectangular	1.73	1	0.10 μHz
Sorption	0.11 μHz	rectangular	1.73	1	0.06 μHz
Change in eccentricity	0.62 μHz	rectangular	1.73	1	0.36 μHz
Expanded uncertainty (k = 1.73)				0.90 μHz	

Table 6. Budget for the expanded combined uncertainty[a] in viscosity (including uncertainties of temperature and pressure) at a temperature of 473.15 K for the (0.75 carbon dioxide + 0.25 nitrogen) mixture.

Source of uncertainty	Uncertainty	Distribution	Coverage factor	Sensitivity coefficient	Standard uncertainty
Viscosity	0.065 μPa·s	normal	2	1	0.033 μPa·s
Pressure	3.5 hPa	rectangular	1.73	0.06 s	$2 \cdot 10^{-5}$ μPa·s
Temperature	162 mK	rectangular	1.73	0.042 μPa·s / K	0.0039 μPa·s
Composition	$1.4 \cdot 10^{-5}$ mol / mol	normal	2	5.4 μPa·s	$3.8 \cdot 10^{-4}$ μPa·s
Expanded combined uncertainty (k = 2)				0.066 μPa·s	

[a] The expanded combined uncertainty ranges from (0.042 to 0.066) μPa·s, depending on temperature for the (0.75 carbon dioxide + 0.25 nitrogen) mixture. This corresponds to a relative expanded combined uncertainty (k = 2) in viscosity of (0.26 to 0.39) %.

Table 7. Experimental (η, p, T) data for nitrogen, presented in the sequence measured, where η is the viscosity, p is the pressure, T is the temperature (ITS-90), $U_c(\eta)$ is the expanded combined uncertainty (k = 2) in viscosity (including uncertainties of temperature[a] and pressure[b]) and ρ_{calc} is the density calculated from the equation of state for nitrogen of Span *et al.* [14].

T / K	p / MPa	ρ_{calc} / (mol·l^{-1})	η / (μPa·s)	$U_c(\eta)$ / (μPa·s)
298.246	1.0001	0.4040	17.893	0.025
298.244	0.8005	0.3233	17.854	0.025
298.246	0.6002	0.2423	17.825	0.025
298.246	0.4007	0.1617	17.797	0.025
298.246	0.2005	0.0809	17.776	0.025
298.246	0.1007	0.0406	17.766	0.025
323.263	1.0009	0.3724	19.007	0.031
323.259	0.8002	0.2977	18.965	0.031
323.260	0.6008	0.2235	18.956	0.031
323.260	0.4004	0.1490	18.926	0.031
323.260	0.2007	0.0747	18.898	0.031
323.261	0.1006	0.0374	18.897	0.031
373.294	1.8072	0.5799	21.222	0.031
373.292	1.5006	0.4819	21.183	0.031
373.294	1.0003	0.3216	21.112	0.031

T / K	p / MPa	ρ_{calc} / (mol·l^{-1})	η / (μPa·s)	$U_c(\eta)$ / (μPa·s)
373.293	0.6010	0.1934	21.074	0.031
373.294	0.4010	0.1291	21.057	0.031
373.293	0.2011	0.0648	21.041	0.031
373.293	0.1008	0.0325	21.023	0.031
423.334	1.7994	0.5082	23.185	0.034
423.333	1.5002	0.4241	23.155	0.034
423.332	1.0005	0.2833	23.112	0.034
423.332	0.6006	0.1703	23.077	0.034
423.332	0.4007	0.1137	23.065	0.034
423.333	0.2009	0.0570	23.034	0.034
423.335	0.1009	0.0286	23.024	0.034
473.382	1.7993	0.4540	25.050	0.036
473.380	1.5006	0.3791	25.032	0.036
473.382	1.0007	0.2533	24.990	0.036
473.381	0.6009	0.1523	24.966	0.036
473.382	0.3985	0.1011	24.965	0.036
473.380	0.2008	0.0510	24.949	0.036
473.380	0.1007	0.0256	24.935	0.036
253.209	1.2009	0.5753	15.837	0.030

T / K	p / MPa	ρ_{calc} / (mol·l^{-1})	η / (μPa·s)	$U_c(\eta)$ / (μPa·s)
253.210	1.0009	0.4788	15.792	0.030
253.210	0.8008	0.3826	15.744	0.030
253.213	0.6008	0.2866	15.706	0.030
253.210	0.4007	0.1909	15.664	0.030
253.211	0.2009	0.0956	15.636	0.030
253.210	0.1008	0.0479	15.612	0.030
273.243	1.4998	0.6642	16.851	0.030
273.240	1.0006	0.4423	16.745	0.030
273.241	0.8006	0.3536	16.710	0.030
273.240	0.6004	0.2650	16.674	0.030
273.239	0.4005	0.1766	16.638	0.030
273.239	0.2008	0.0885	16.615	0.030
273.240	0.1007	0.0444	16.592	0.030
		Reproducibility checks		
298.252	1.5002	0.6064	17.985	0.025
298.251	1.0001	0.4040	17.894	0.025
298.249	0.4008	0.1617	17.799	0.025
298.249	0.0996	0.0402	17.762	0.025
323.268	1.8021	0.6703	19.127	0.031
323.267	1.5019	0.5587	19.075	0.031

T / K	p / MPa	ρ_{calc} / (mol·l^{-1})	η / (μPa·s)	$U_c(\eta)$ / (μPa·s)
323.264	1.0006	0.3723	19.008	0.031
323.266	0.3988	0.1484	18.929	0.031
323.265	0.1015	0.0378	18.902	0.031

[a] The expanded uncertainties (k = 1.73) of the temperature at T = (253.15, 273.15, 298.15, 323.15, 373.15, 423.15, 473.15) K are $U(T)$ = (104, 108, 111, 112, 121, 136, 162) mK, respectively.

[b] The expanded uncertainty (k = 1.73) of the pressure is $U(p)$ = 3.5 hPa.

Table 8. Coefficients for the limit of zero density, $\eta_{\mathrm{exp}}^{(0)}$, and for the second viscosity virial coefficient B_η for nitrogen.

T / K	$\eta_{\mathrm{exp}}^{(0)}$ / (μPa·s)	B_η / (l·mol^{-1})
298.246	17.747	0.0193
323.261	18.879	0.0169
373.293	21.010	0.0172
423.333	23.019	0.0142
473.381	24.932	0.0103
253.210	15.589	0.0270
273.240	16.570	0.0247
Reproducibility checks		
298.250	17.740	0.0223
323.266	18.881	0.0188

Table 9. Selected experimental viscosity data of nitrogen.

Author	Type of viscometer	Temperature range in K	Pressure range in MPa	Claimed uncertainty in %
Clarke and Smith [15]	Capillary	120−360	0.1	
DiPippo *et al.* [16]	Oscillating-disk	303	0.1−2.3	
Docter *et al.* [8]	Rotating-cylinder	253−523	0.1−28.5	0.4
El Hawary [10]	Rotating-cylinder	253−473	0.1−20.0	0.07−0.5
Evers *et al.* [9]	Rotating-cylinder	233−523	0.1−29.7	0.15−0.6
Flynn *et al.* [17]	Capillary	195−373	0.6−17.9	0.1
Gough *et al.* [18]	Capillary	120−320	0.1	0.5−1.0
Gracki *et al.* [19]	Capillary	183−298	0.5−25.7	0.1−0.2
Hellemans *et al.* [20]	Oscillating-disk	298−767	0.1	0.1−0.3
Kestin *et al.* [21]	Oscillating-disk	303	0.1−2.6	0.1
Kestin *et al.* [22]	Oscillating-disk	298	0.1−10.7	0.2
Kestin *et al.* [23]	Oscillating-disk	298−973	0.1	0.1−0.3
Kestin *et al.* [24]	Oscillating-disk	298−673	0.1	0.1−0.2
May *et al.* [25]	Capillary	298	0.1	0.09
Seibt *et al.* [26]	Vibrating-wire	298-423	0.1-22	0.2-0.3
Seibt *et al.* [27]	Vibrating-wire	293−423	0.1	0.2−0.3
Vogel [28]	Oscillating-disk	291−682	0.1	0.15−0.2

Table 10. Experimental (η, p, T) data for three (carbon dioxide + nitrogen) mixtures, presented in the sequence measured, where η is the viscosity, p is the pressure, T is the temperature (ITS-90), $U_c(\eta)$ is the expanded combined uncertainty (k = 2) in viscosity (including uncertainties of temperature[a] and pressure[b]) and ρ_{calc} is the density calculated from the GERG-2008 EOS implemented in REFPROP 9.1 [[33],[4]].

T / K	p / MPa	ρ_{calc} /(mol·l^{-1})	η / (μPa·s)	$U_c(\eta)$ / (μPa·s)
		x_{N_2} = 0.74981		
298.191	1.4984	0.6138	17.442	0.044
298.192	0.9993	0.4073	17.339	0.044
298.192	0.8010	0.3258	17.302	0.044
298.191	0.6042	0.2453	17.265	0.044
298.192	0.4023	0.1630	17.242	0.044
298.193	0.1967	0.0795	17.208	0.044
298.193	0.1089	0.0440	17.191	0.044
323.205	1.5001	0.5640	18.604	0.051
323.203	1.0009	0.3751	18.504	0.051
323.201	0.8003	0.2995	18.473	0.051
323.203	0.6002	0.2243	18.441	0.051
323.203	0.3938	0.1470	18.414	0.051
323.202	0.1982	0.0738	18.380	0.051
323.203	0.1091	0.0406	18.366	0.051

T / K	p / MPa	ρ_{calc} /(mol·l^{-1})	η / (μPa·s)	$U_c(\eta)$ / (μPa·s)
373.570	2.0419	0.6605	20.907	0.053
373.570	1.5012	0.4851	20.807	0.053
373.571	1.0024	0.3235	20.732	0.053
373.570	0.5982	0.1929	20.684	0.053
373.573	0.3993	0.1287	20.654	0.053
373.569	0.1992	0.0642	20.635	0.053
373.569	0.1088	0.0350	20.614	0.053
423.267	2.0000	0.5682	22.933	0.059
423.267	1.5001	0.4262	22.866	0.059
423.268	1.0003	0.2843	22.808	0.059
423.266	0.6007	0.1707	22.754	0.059
423.269	0.3987	0.1133	22.736	0.059
423.272	0.2004	0.0569	22.716	0.059
423.269	0.1089	0.0309	22.710	0.059
473.313	1.9967	0.5058	24.886	0.063
473.313	1.5014	0.3807	24.821	0.063
473.313	1.0038	0.2547	24.774	0.063
473.314	0.6028	0.1530	24.739	0.063
473.312	0.3990	0.1013	24.718	0.063

T / K	p / MPa	ρ_{calc} /(mol·l^{-1})	η / (μPa·s)	$U_c(\eta)$ / (μPa·s)
473.315	0.1990	0.0506	24.707	0.063
473.313	0.1087	0.0276	24.698	0.063
253.165	0.9984	0.4843	15.142	0.046
253.165	0.7971	0.3850	15.086	0.046
253.165	0.6011	0.2892	15.047	0.046
253.165	0.3990	0.1911	15.007	0.046
253.164	0.2031	0.0969	14.975	0.046
253.166	0.1003	0.0478	14.954	0.046
273.190	1.2006	0.5384	16.186	0.047
273.190	1.0001	0.4471	16.134	0.047
273.190	0.8002	0.3567	16.099	0.047
273.190	0.6003	0.2667	16.054	0.047
273.190	0.4017	0.1779	16.023	0.047
273.190	0.2010	0.0888	15.986	0.047
273.189	0.1088	0.0480	15.967	0.047
		Reproducibility checks		
298.204	1.5014	0.6150	17.438	0.044
298.205	1.0085	0.4110	17.340	0.044
298.205	0.8070	0.3282	17.300	0.044
298.203	0.5996	0.2434	17.275	0.044

T / K	p / MPa	ρ_{calc} /(mol·l^{-1})	η / (μPa·s)	$U_c(\eta)$ / (μPa·s)
298.205	0.3905	0.1581	17.240	0.044
298.203	0.2026	0.0819	17.203	0.044
298.206	0.1090	0.0440	17.193	0.044
		x_{N_2} = 0.49962		
298.208	1.2020	0.4977	16.696	0.031
298.207	1.0000	0.4122	16.641	0.031
298.207	0.8009	0.3287	16.599	0.031
298.206	0.5934	0.2425	16.563	0.031
298.208	0.3991	0.1624	16.542	0.031
298.206	0.2047	0.0829	16.502	0.031
298.207	0.1080	0.0437	16.496	0.031
323.218	1.1986	0.4545	17.870	0.042
323.217	0.9964	0.3767	17.826	0.042
323.218	0.8049	0.3034	17.798	0.042
323.219	0.5980	0.2246	17.765	0.042
323.216	0.3986	0.1493	17.727	0.042
323.218	0.2009	0.0750	17.703	0.042
323.220	0.1092	0.0407	17.686	0.042
373.246	1.4980	0.4887	20.199	0.040

T / K	p / MPa	ρ_{calc} /(mol·l^{-1})	η / (μPa·s)	$U_c(\eta)$ / (μPa·s)
373.245	0.9986	0.3245	20.112	0.040
373.246	0.7995	0.2594	20.081	0.040
373.246	0.5985	0.1938	20.054	0.040
373.246	0.3913	0.1265	20.021	0.040
373.245	0.2007	0.0648	19.999	0.040
373.247	0.1078	0.0348	19.978	0.040
423.279	1.9950	0.5714	22.422	0.045
423.277	1.4965	0.4278	22.331	0.045
423.279	1.0017	0.2858	22.264	0.045
423.278	0.6030	0.1718	22.210	0.045
423.280	0.4000	0.1138	22.189	0.045
423.280	0.1999	0.0568	22.160	0.045
423.280	0.1094	0.0311	22.155	0.045
473.322	1.9919	0.5076	24.438	0.048
473.320	1.5030	0.3828	24.370	0.048
473.325	1.0062	0.2561	24.314	0.048
473.322	0.6024	0.1532	24.267	0.048
473.323	0.4001	0.1017	24.244	0.048
473.322	0.2037	0.0518	24.230	0.048
473.324	0.1081	0.0275	24.217	0.048

T / K	p / MPa	ρ_{calc} /(mol·l^{-1})	η / (μPa·s)	$U_c(\eta)$ / (μPa·s)
253.168	0.7988	0.3918	14.350	0.042
253.168	0.5962	0.2900	14.310	0.042
253.169	0.3983	0.1922	14.274	0.042
253.169	0.2004	0.0960	14.245	0.042
253.170	0.1081	0.0516	14.230	0.042
273.197	1.0045	0.4559	15.414	0.042
273.195	0.8001	0.3609	15.372	0.042
273.194	0.6031	0.2704	15.333	0.042
273.193	0.4009	0.1786	15.299	0.042
273.196	0.2056	0.0911	15.267	0.042
273.195	0.1092	0.0482	15.249	0.042
		Reproducibility checks		
298.209	1.2044	0.4987	16.692	0.031
298.210	1.0033	0.4136	16.639	0.031
298.210	0.8036	0.3298	16.606	0.031
298.209	0.6038	0.2468	16.567	0.031
298.208	0.4023	0.1637	16.535	0.031
298.209	0.2019	0.0818	16.509	0.031
298.210	0.1090	0.0441	16.493	0.031

T / K	p / MPa	ρ_{calc} /(mol·l^{-1})	η / (μPa·s)	$U_c(\eta)$ / (μPa·s)
		x_{N_2} = 0.24788		
298.211	1.0024	0.4193	15.849	0.042
298.210	0.8076	0.3354	15.809	0.042
298.209	0.6029	0.2485	15.769	0.042
298.207	0.3951	0.1616	15.742	0.042
298.209	0.2052	0.0834	15.718	0.042
298.210	0.1087	0.0440	15.710	0.042
323.221	1.1968	0.4600	17.096	0.055
323.221	1.0018	0.3830	17.050	0.055
323.220	0.7989	0.3038	17.015	0.055
323.222	0.6050	0.2288	16.979	0.055
323.220	0.3994	0.1502	16.951	0.055
323.221	0.1961	0.0734	16.928	0.055
323.220	0.1084	0.0405	16.914	0.055
373.246	1.4982	0.4942	19.466	0.055
373.250	0.9996	0.3272	19.367	0.055
373.245	0.8022	0.2617	19.331	0.055
373.248	0.6015	0.1956	19.301	0.055
373.249	0.4006	0.1299	19.278	0.055
373.248	0.2001	0.0647	19.248	0.055

T / K	p / MPa	ρ_{calc} /(mol·l^{-1})	η / (μPa·s)	$U_c(\eta)$ / (μPa·s)
373.248	0.1033	0.0333	19.234	0.055
423.289	1.9985	0.5782	21.751	0.062
423.286	1.4951	0.4306	21.652	0.062
423.286	1.0007	0.2870	21.557	0.062
423.288	0.6011	0.1717	21.507	0.062
423.288	0.4051	0.1155	21.478	0.062
423.289	0.2014	0.0573	21.450	0.062
423.284	0.1077	0.0306	21.437	0.062
473.339	1.9985	0.5130	23.816	0.066
473.342	1.4954	0.3829	23.727	0.066
473.341	1.0004	0.2555	23.653	0.066
473.343	0.5973	0.1523	23.589	0.066
473.344	0.3958	0.1008	23.578	0.066
473.343	0.2031	0.0517	23.556	0.066
473.343	0.1093	0.0278	23.548	0.066
253.179	0.6052	0.2990	13.516	0.053
253.180	0.3963	0.1931	13.484	0.053
253.180	0.2037	0.0980	13.475	0.053
253.180	0.1104	0.0528	13.467	0.053

T / K	p / MPa	ρ_{calc} /(mol·l^{-1})	η / (μPa·s)	$U_c(\eta)$ / (μPa·s)
273.206	0.7939	0.3636	14.571	0.053
273.205	0.6016	0.2728	14.534	0.053
273.205	0.3979	0.1786	14.504	0.053
273.205	0.2011	0.0894	14.483	0.053
273.207	0.1081	0.0478	14.475	0.053
		Reproducibility checks		
298.222	1.0030	0.4196	15.848	0.042
298.222	0.7946	0.3298	15.812	0.042
298.219	0.6021	0.2482	15.777	0.042
298.222	0.4012	0.1641	15.749	0.042
298.223	0.2048	0.0832	15.724	0.042
298.221	0.1079	0.0437	15.706	0.042

[a] The expanded uncertainties (k = 1.73) of the temperature at T = (253.15, 273.15, 298.15, 323.15, 373.15, 423.15, 473.15) K are $U(T)$ = (104, 108, 111, 112, 121, 136, 162) mK, respectively.

[b] The expanded uncertainty (k = 1.73) of the pressure is $U(p)$ = 3.5 hPa.

Table 11. Coefficients for the viscosity in the limit of zero density, $\eta_{exp}^{(0)}$, and for the second viscosity virial coefficient B_η for three (carbon dioxide + nitrogen) mixtures.

T / K	$\eta_{exp}^{(0)}$ /(μPa·s)	B_η /(l·mol^{-1})	T / K	$\eta_{exp}^{(0)}$ /(μPa·s)	B_η /(l·mol^{-1})
	x_{N_2} = 0.74981			x_{N_2} = 0.24788	
298.192	17.169	0.0251	298.209	15.686	0.0236
323.203	18.345	0.0243	323.221	16.892	0.0249
373.570	20.597	0.0219	373.248	19.211	0.0257
423.268	22.690	0.0184	423.287	21.412	0.0265
473.313	24.682	0.0155	473.342	23.522	0.0234
253.165	14.931	0.0281	253.180	13.455	0.0140
273.190	15.944	0.0274	273.206	14.456	0.0209
	Reproducibility check			Reproducibility check	
298.204	17.170	0.0250	298.222	15.670	0.0237
	x_{N_2} = 0.49962				
298.207	16.468	0.0261			
323.218	17.667	0.0246			
373.246	19.962	0.0238			
423.279	22.131	0.0221			
473.323	24.201	0.0188			
253.169	14.210	0.0246			
273.195	15.228	0.0263			
	Reproducibility check				
298.209	16.469	0.0259			

Table 12. Coefficients in equation (18) for the temperature-dependent second pressure virial coefficients.

Coefficient	CO_2	N_2
α_i / (cm³·mol^{-1})	134.46	167.42
β_i / (cm³·mol^{-1})	−85.08	−123.30
γ_i / K	330.47	99.84

Table 13. Coefficients $a_{i,k}$, and $b_{i,k}$ in equations (21) and (23) for calculation of the effective hard-sphere diameters σ_i^0 and σ_i^χ, and binary interaction parameter L_{12} in equation (22) for σ_{ij}^0, where i = 1 for carbon dioxide and i = 2 for nitrogen.

k	$a_{1,k}$	$a_{2,k}$	L_{12}	$b_{1,k}$	$b_{2,k}$
0	0.66723	0.49920	$2.1470\cdot10^{-2}$	1.41158	0.26844
1	$-1.1959\cdot10^{-3}$	$-7.8369\cdot10^{-4}$		$-4.2825\cdot10^{-3}$	$5.3053\cdot10^{-5}$
2	$1.9693\cdot10^{-6}$	$1.5048\cdot10^{-6}$		$4.4484\cdot10^{-6}$	$1.3028\cdot10^{-7}$
3	$-1.2319\cdot10^{-9}$	$-1.0759\cdot10^{-9}$			

FIGURE CAPTIONS

Figure 1. Relative deviations of experimental viscosities η_{exp} for nitrogen from values η_{calc} calculated with the correlation of Lemmon *et al.* [2] (zero line). Deviations are plotted *vs.* density ρ calculated with the equation of state of Span *et al.* [14]. •, This work; ▪, DiPippo *et al.* [16]; ×, Docter *et al.* [8]; ○, El Hawary [10]; ▵, Evers *et al.* [9]; ◇, Flynn *et al.* [17]; ⊠, Gough *et al.* [18]; ⊠, Gracki *et al.* [19]; ◇, Hellemans *et al.* [20]; +, Kestin *et al.* [23]; ▬, Kestin *et al.* [21]; ▫, Kestin *et al.* [22]; ■, Kestin *et al.* [24]; ○, May *et al.* [25]; ◆, Seibt *et al.* [26]; ⋆, Seibt *et al.* [27]; □, Vogel [28].

Figure 2. Relative deviations of experimental viscosities η_{exp} for nitrogen from values η_{calc} calculated with the correlation of Lemmon *et al.* [2] (zero line). Deviations are plotted *vs.* density ρ calculated with the equation of state of Span *et al.* [14]. •, This work; ×, Docter *et al.* [8]; ○, El Hawary [10]; ▵, Evers *et al.* [9]; ◇, Hellemans *et al.* [20]; +, Kestin *et al.* [23]; ■, Kestin *et al.* [24]; ◆, Seibt *et al.* [26]; ⋆, Seibt *et al.* [27]; □, Vogel [28].

Figure 3. Relative deviations of zero-density viscosities $\eta_{exp}^{(0)}$ for nitrogen from values η_{calc} calculated with the correlation of Lemmon *et al.* [2] (zero line). Deviations are plotted *vs.* temperature *T*. •, This work (extrapolated to zero density); ▵, Berg and Moldover [31]; ▲, Clarke and Smith [15]; ⋯▬⋯ , Cole and Wakeham [32]; ▪, DiPippo *et al.* [16]; ○, El Hawary [10]; ▵, Evers *et al.* [9]; ⊠, Gough *et al.* [18]; ⊠, Gracki *et al.* [19]; ▬ · ▬, Hellmann [29]. ▪▪▪▪▪ , Hellmann [29] (scaled by 1.0024); ▬, Kestin *et al.* [21]; ▫, Kestin *et al.* [22]; ○, May *et al.* [25]; ◆, Seibt *et al.* [26]; ⋆, Seibt *et al.* [27]; □, Vogel [28].

Figure 4. Relative deviations of experimental viscosities η_{exp} for three (carbon dioxide + nitrogen) mixtures from values η_{calc} calculated with the ECS model [5] implemented in REFPROP 9.1 [3] (zero line). Deviations are plotted *vs.* density ρ calculated with the GERG-2008 equation of state [33] implemented in REFPROP 9.1 [4]. ◆, 298.15 K; □, 323.15 K; ✶, 373.15 K; ▲, 423.15 K; ○, 473.15 K; △, 253.15 K; ●, 273.15 K; ◇, 298.15 K (Reproducibility checks).

Figure 5. Relative deviations of experimental viscosities η_{exp} for three (carbon dioxide + nitrogen) mixtures from values η_{calc} calculated with the ECS model [5] implemented in REFPROP 9.1 [3] (zero line) near room temperature. Deviations are plotted *vs.* density ρ calculated with the GERG-2008 equation of state [33] implemented in REFPROP 9.1 [4]. ◆, This work; ◇, This work (Reproducibility checks); ○, Kestin and Leidenfrost [34]; △, Kestin and Ro [35]; □, Kestin *et al.* [21].

Figure 6. Relative deviations of viscosities in the limit of zero density $\eta_{exp}^{(0)}$ for three (carbon dioxide + nitrogen) mixtures from values η_{calc} calculated with the ECS model [5] implemented in REFPROP 9.1 [3] (zero line). Deviations are plotted *vs.* temperature *T*. ◇, x_{N2} = 0.24788; △, x_{N2} = 0.49962; ○, x_{N2} = 0.74981; ..... , Crusius *et al.* [36] x_{N2} = 0.25; – – –, Crusius *et al.* [36] x_{N2} = 0.5; – · –, Crusius *et al.* [36] x_{N2} = 0.75. For clarity we have only plotted the error bars for the equimolar mixture but the error bars of the other compositions are, however, alike. Please note: For better traceability we have taken the original calculated values by Crusius *et al.* [36] without any scaling. The deviations of this work's data to the recommended data of Crusius *et al.* [36] are, however, similar but with negative sign.

Figure 7. Relative deviations of viscosities in the limit of zero density $\eta_{\mathrm{exp}}^{(0)}$ for three (carbon dioxide + nitrogen) mixtures and the pure fluids nitrogen and carbon dioxide from values $\eta_{\mathrm{calc}}^{(0)}$ calculated with the Hendl and Vogel scheme [6]. Deviations are plotted *vs.* temperature *T*. ×, x_{N2} = 0; ⋄, x_{N2} = 0.24788; ▵, x_{N2} = 0.49962; ○, x_{N2} = 0.7498; □, x_{N2} = 1.

Figure 8. Relative deviations of experimental viscosities η_{exp} for three (carbon dioxide + nitrogen) mixtures from values η_{calc} calculated with the Hendl and Vogel scheme [6]. Deviations are plotted *vs.* density ρ calculated with the GERG-2008 equation of state [33] implemented in REFPROP 9.1 [4]. ◆, 298.15 K; □, 323.15 K; ✶, 373.15 K; ▲, 423.15 K; ○, 473.15 K; ▵, 253.15 K; ●, 273.15 K.

Figure 9. Relative deviations of experimental viscosities η_{exp} for nitrogen and carbon dioxide [1] from values η_{calc} calculated with the Hendl and Vogel scheme [6]. Deviations are plotted *vs.* density ρ calculated with the equation of state of Span *et al.* [14] (nitrogen) and Span and Wagner [42] (carbon dioxide). ◆, 298.15 K; □, 323.15 K; ✶, 373.15 K; ▲, 423.15 K; ○, 473.15 K; ▵, 253.15 K; ●, 273.15 K.

Figure 1

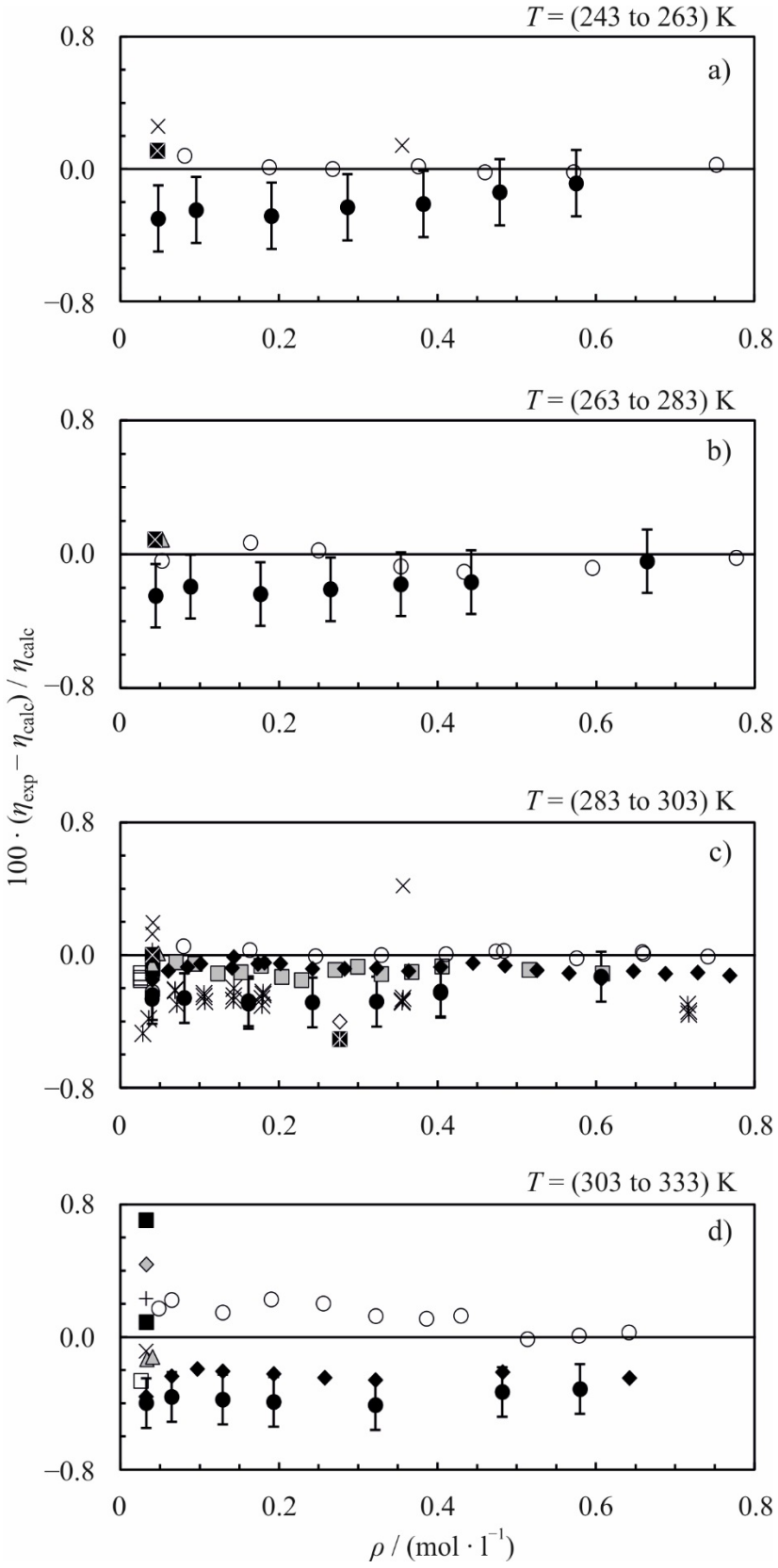

T = (243 to 263) K
a)
T = (263 to 283) K
b)
T = (283 to 303) K
c)
T = (303 to 333) K
d)
0.8
0.0
−0.8
0
0.2
0.4
0.6
0.8
100 · (η_exp − η_calc) / η_calc
ρ / (mol · l^−1)

Figure 2

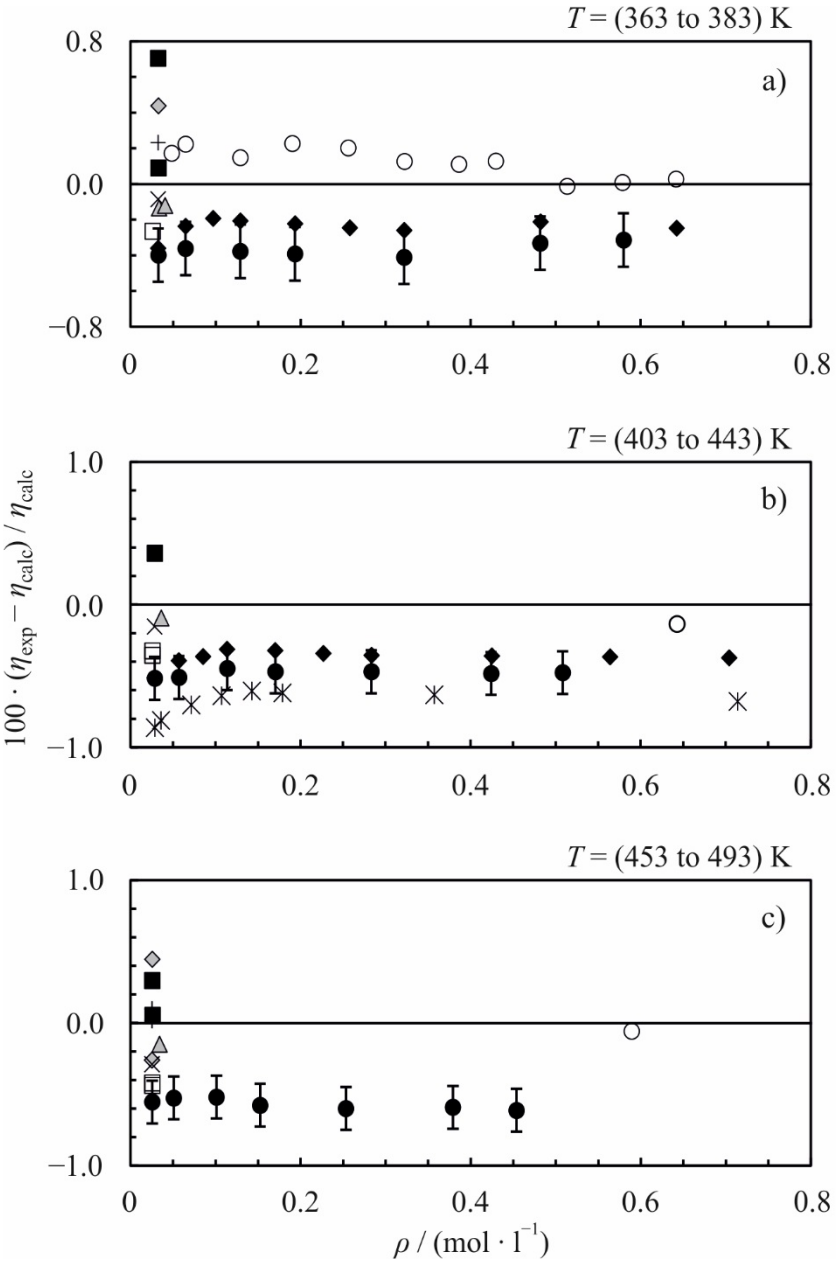

T = (363 to 383) K
a)
T = (403 to 443) K
b)
T = (453 to 493) K
c)
100 · (η_exp − η_calc) / η_calc
ρ / (mol · l^−1)

Figure 3

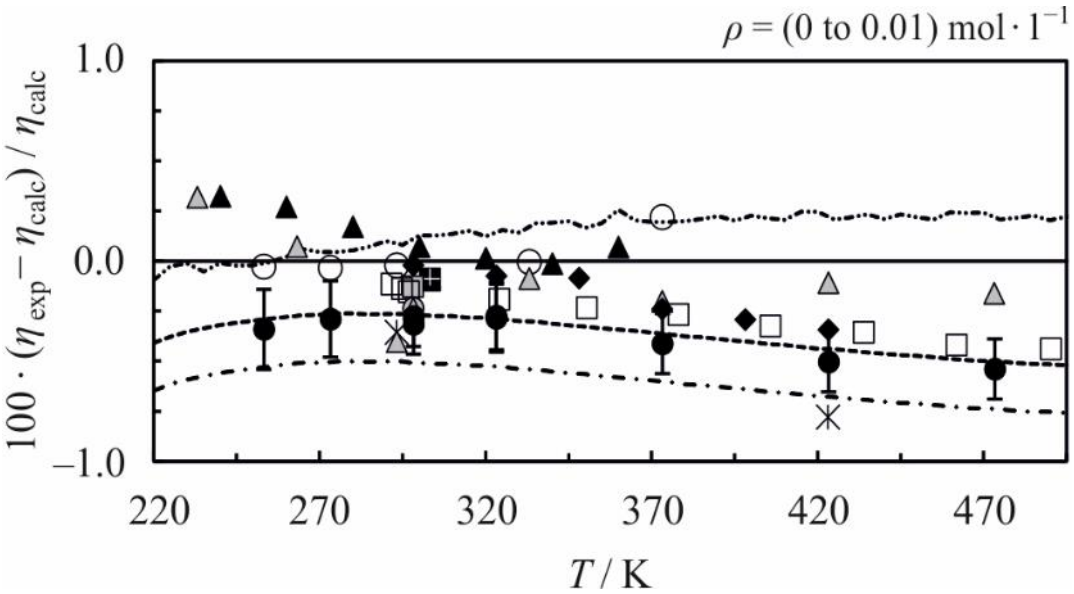

ρ = (0 to 0.01) mol · l⁻¹
100 · (η exp − η calc) / η calc
1.0
0.0
–1.0
220
270
320
370
420
470
T / K

Figure 4

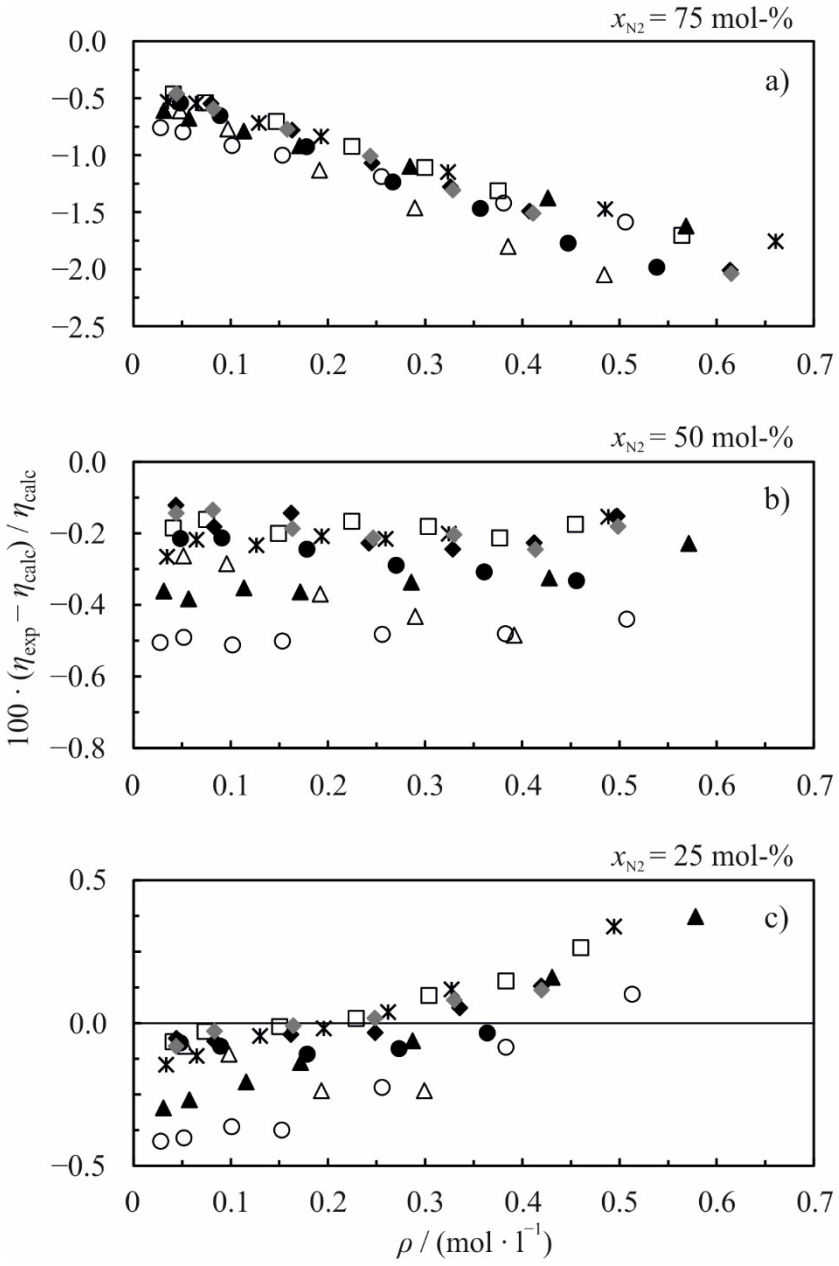

x_{N2} = 75 mol-%
a)
x_{N2} = 50 mol-%
b)
x_{N2} = 25 mol-%
c)
$100 \cdot (\eta_{exp} - \eta_{calc}) / \eta_{calc}$
ρ / (mol · l^{-1})

Figure 5

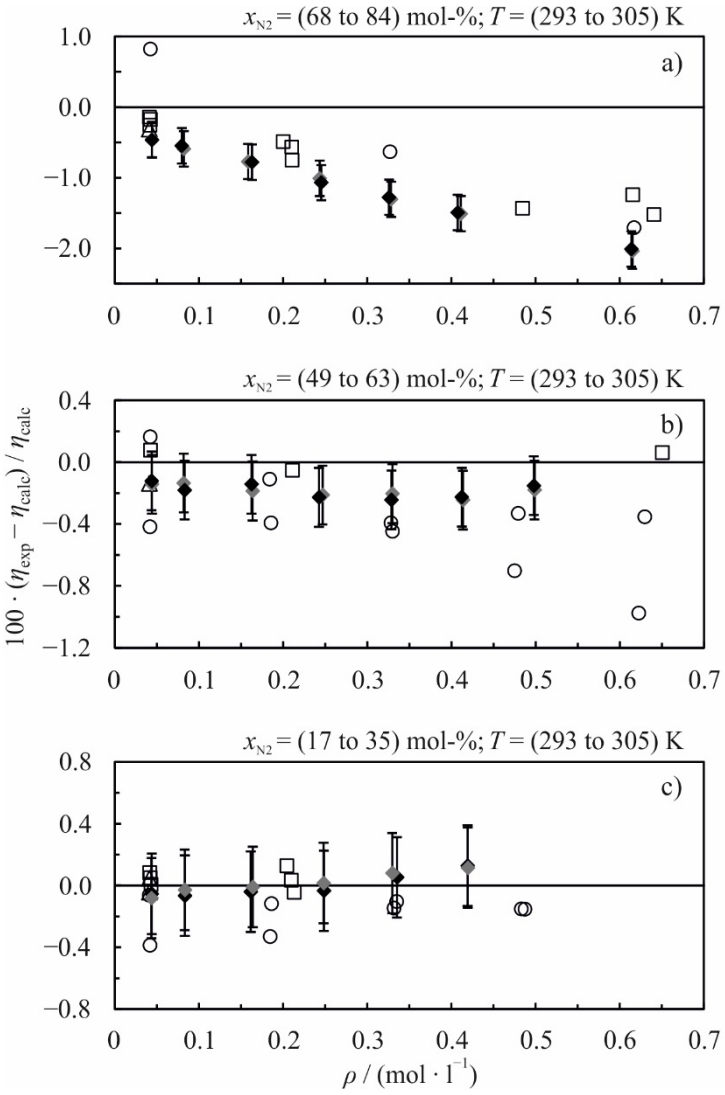

x_{N2} = (68 to 84) mol-%; T = (293 to 305) K
a)
x_{N2} = (49 to 63) mol-%; T = (293 to 305) K
b)
x_{N2} = (17 to 35) mol-%; T = (293 to 305) K
c)
$100 \cdot (\eta_{exp} - \eta_{calc}) / \eta_{calc}$
ρ / (mol · l^{-1})

Figure 6

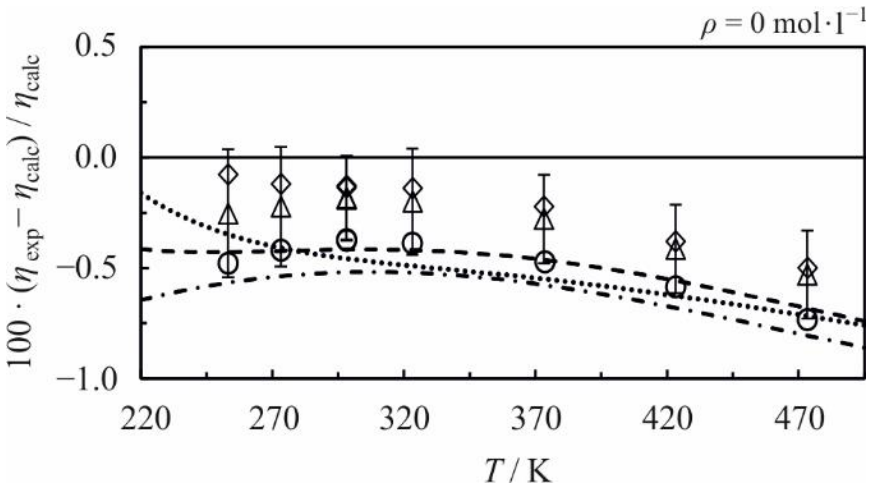


Figure 7

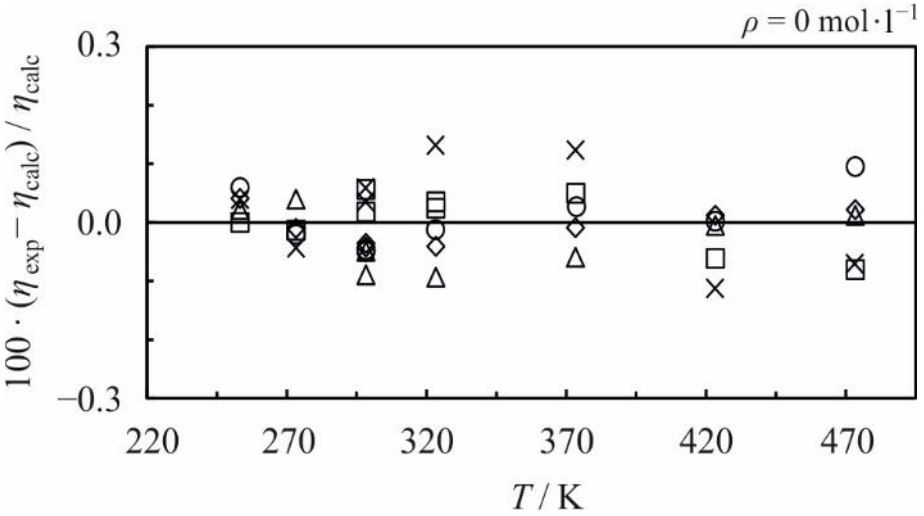


Figure 8

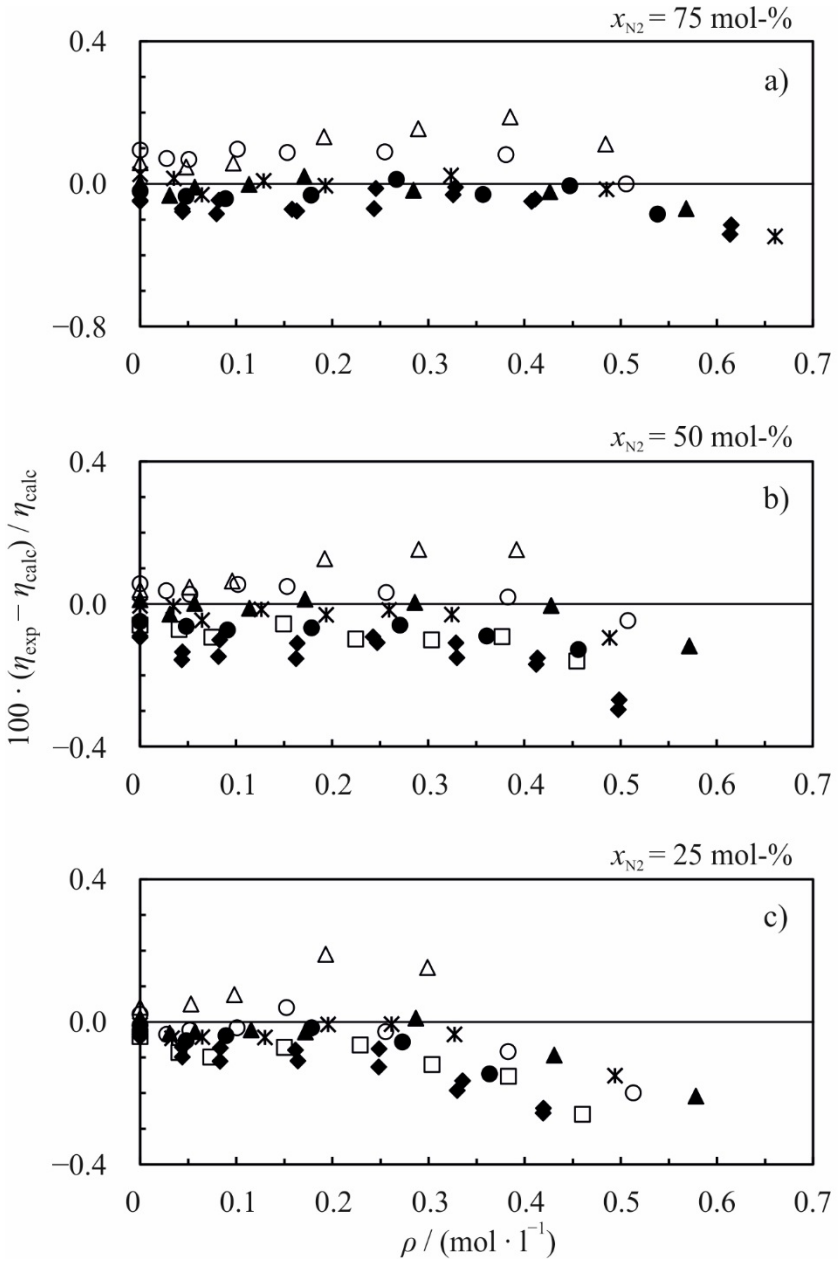
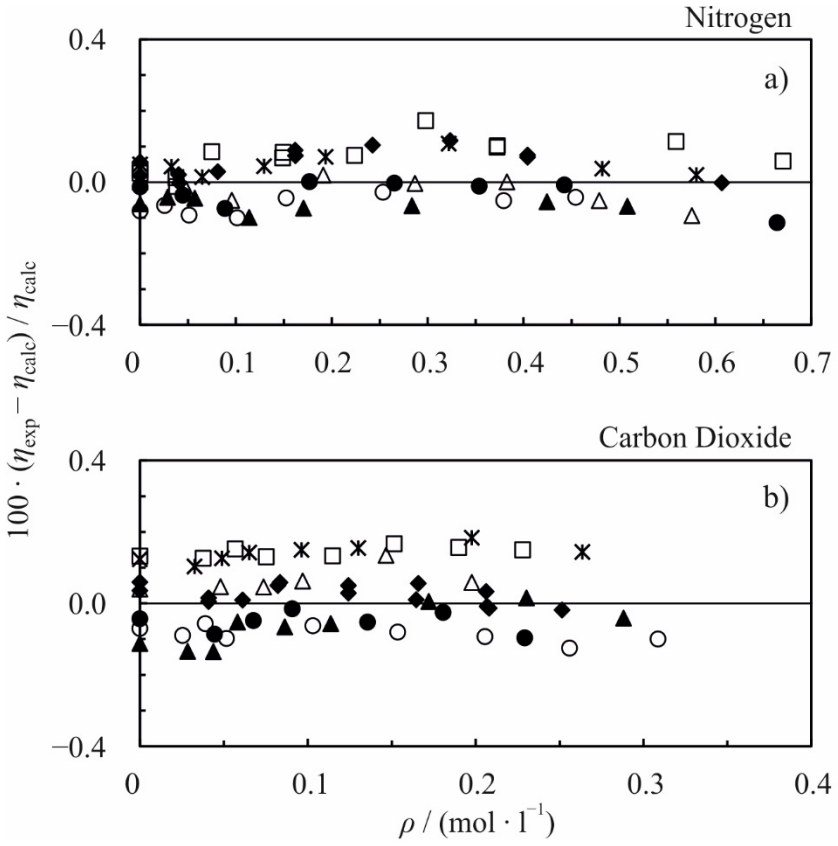

x_{N2} = 75 mol-%
a)
x_{N2} = 50 mol-%
b)
x_{N2} = 25 mol-%
c)
$100 \cdot (\eta_{exp} - \eta_{calc}) / \eta_{calc}$
ρ / (mol · l^{-1})
0.4
0.0
−0.8
−0.4
0
0.1
0.2
0.3
0.4
0.5
0.6
0.7

Figure 9


Nitrogen
a)
0.4
0.0
−0.4
0
0.1
0.2
0.3
0.4
0.5
0.6
0.7
Carbon Dioxide
b)
0.4
0.0
−0.4
0
0.1
0.2
0.3
0.4
$100 \cdot (\eta_{exp} - \eta_{calc}) / \eta_{calc}$
ρ / (mol · l^{-1})